Statement of Problem

Coronal Mass Ejections and their interplanetary counterparts (ICMEs) are among the most powerful and potentially hazardous phenomena in the Earth's near space environment. ICMEs are capable of generating geomagnetic storms in the magnetosphere of the Earth and are the major driver of space weather, with negative effects ranging from the disruption of power grids, damage to satellites in orbit and interference in radio and other communication systems. As human civilization continues to become increasingly dependent on technology, an ability to predict when these eruptions may impact the Earth and the severity of the ensuing storm could help to prevent damage (Pulkkinen, 2007; Bala et al., 2015).

The major goal of this proposal will be the development of improved tools for the tracking and measurement of both a Coronal Mass Ejection (CME) ejecta and the sheath of accumulated plasma and possible shock wave in front of it. By creating more advanced tools that can more accurately determine the location and evolution of each front, the space physics community will benefit by having more accurate inputs for forecasting and analytical models and having and improved understanding of the independent structures associated with a CME. This is an important distinction to make when considering the space weather impacts of an eruption, as the ejecta will have more importance for generating powerful geomagnetic storms but the associated shock waves can generate Solar Energetic Particles (SEPs), another space weather hazard.

Background and Relevance to Previous Work

To comprehend how a CME propagates, a proper understanding of the full CME structure is necessary. While debate remains about the initiation mechanism of a CME, it is widely believed that the actual structure that erupts from the corona into the heliosphere is a magnetic flux rope (Vourlidas et al., 2013; Zhang et al., 2013). I will be focusing primarily on the CME in the heliosphere, and therefore the exact process of CME initiation, while an important scientific subject, will not be considered in this proposal.

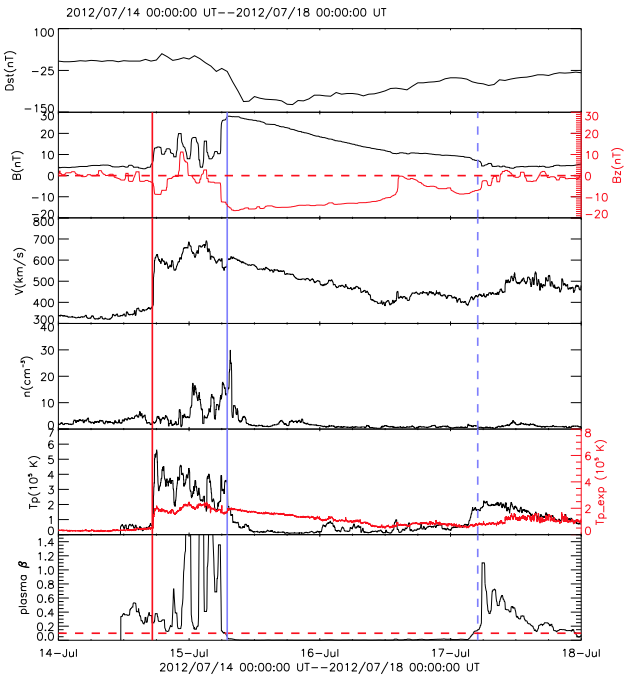

Figure 1: Solar Wind data measured by ACE between July 14 and July 18, 2012. The shock onset is denoted with the red line, the ejecta onset with the solid blue line and the passing of the ejecta with the dotted blue line. Plots from top to bottom show the Dst index, total magnetic field and the z component of the magnetic field (red), total velocity, density, temperature and the expected temperature (red) based on the velocity, and the plasma β.

The internal magnetic field of the CME, also called the ejecta or driver, will be much stronger than that of the ambient solar wind causing a pressure imbalance with the solar wind such that the CME will expand as it propagates. The CME will expand from the initial size of a few tenths of a R to an average size of 0.3 AU by the time it reaches the Earth (Zhang et al., 2008). At the L1 point near the Earth, the Advanced Composition Explorer (ACE) spacecraft takes in-situ measurements of solar wind plasma parameters like temperature, density and velocity as well as measurements of the complete vector magnetic field (Stone et al., 1998). These observations allow for the detection of different signatures for both the driven shock (if there is one), sheath region and the ejecta, commonly seen as a so-called magnetic cloud (Burlaga et al., 1981; Lepping et al., 1990; Li et al., 2014). If this structure has a magnetic field pointing strongly to the south, it will undergo magnetic reconnection with the northward magnetic field of the Earth, opening the magnetopause and allowing energy to be deposited into the Earth's magnetosphere.

The sheath is important for study, as it will be the first structure to reach the Earth and it can also cause some reconnection. However, the bulk of the energy in a geomagnetic storm comes from the ejecta portion of the CME. On average, the sheath has been observed to be responsible for 30% of the energy deposited during a geomagnetic event (Zhang et al., 2008). An in-situ plot showing the signatures of a shock, sheath and ejecta is shown in Figure 1.

If the ejecta driving the sheath is traveling faster than the local Alfvén speed, a shock

wave will be formed. These shock waves are, independently of the ejecta, important for space weather research because of the generation of Solar Energetic Particles (SEPs). SEPs can cause many harmful effects, including endangering the lives of astronauts and damaging spacecraft. They are often associated with the passage of a CME driven shock wave through a magnetic field line connected to the Earth (or another observer) (Gopalswamy et al., 2014; Kozarev et al., 2015). To understand SEPs, it is important to understand the exact geometry and location of all parts of the shock front, making a careful study of a shocks vital for solar research and space weather forecasting.

Many works dealing with CME evolution have failed to deal with these different regions separately, and have instead treated the entire CME-Sheath system as one structure. This is problematic, as it is important to know the time of arrival each front separately, but in order to truly understand the physics which govern their evolution, it is necessary to separate the two structures and study how they propagate independently and how they interact. In my previous work on CME propagation and all planned work in this proposal, I carefully separate the shock and ejecta structure and consider the evolution of each front individually.

General Methodology and Procedures

By combining white-light images from the SOHO and STEREO satellites, a CME can be observed in Thompson scattered white light from three viewpoints. My primary method for making measurements is a forward modeling technique that works by superimposing a three-dimensional geometric structure onto the observations to determine the parameters that best recreate the observed features. I use the Graduated Cylindrical Shell (GCS) model developed by Thernisien et al. (2006, 2009) which mimics the structure of a magnetic flux rope. This is a geometric model defined by six free parameters that control the shape of the ejecta, and has been successfully used to study the dynamics of many CMEs (Poomvises et al., 2010; Colaninno et al., 2013). For the sheath, I use a spheroid "bubble model", similar that used by Kwon et al. (2014). Figure 2 shows both models fit to observations.

Using these models over a number of time steps, I can obtain a series of height-time measurements. In order to determine the kinematics of the CME, it is more accurate to fit the height-time data to a known function and compute an analytical derivative rather than a numerical derivate to the measurements (Byrne et al., 2013).

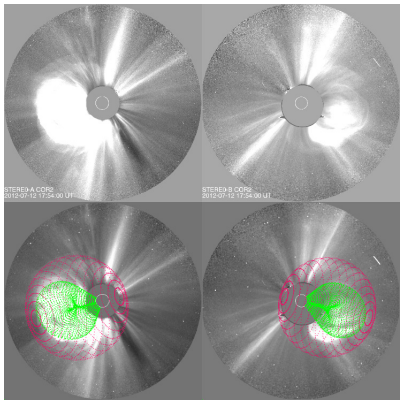

Figure 2: Model fitting of CME ejecta and shock front. Images at 17:54 UT on July 12, 2012 from STEREO A COR2 (Left) and STEREO B COR2 (Right) are shown along without (top) and with (bottom) the model mesh. The green mesh shows the GCS fitting to the CME ejecta, while the red mesh shows the spheroid fitting to the CME shock front.

It has been well established that regardless of initial velocity, the speed of a CME will gradually trend towards that of the ambient solar wind, in most cases before it reaches the Earth (Sheeley et al., 1999). CMEs that are initially faster than the solar wind speed will decelerate, while slower CMEs will be pushed by the solar wind and accelerate. The main assumption of drag models (Cargill, 2004; Vršnak et al., 2013) is that the significant controlling factor of the deceleration of a fast CME to the speed of the solar wind is aerodynamic drag. The height function of the drag model I have used is (Hess & Zhang, 2014)

$$r(t) = \frac{1}{\Gamma} ln[1 + \Gamma(v_0 - v_{sw})t] + v_{sw}t + r_0 \tag{1}$$

v_0 is the initial speed of the CME and r_0 is its initial height, both of which can be obtained reliably from measurement. v_{sw} is the the solar wind speed, which can be measured in-situ ahead of the CME arrival at 1 AU and is treated as a constant value in the heliosphere; leaving one unconstrained term, Γ, the drag parameter which controls the deceleration rate.

Explanation of New or Unique Techniques

Observationally both the CME and its shock front can be seen in white light in the heliosphere. (Ontiveros & Vourlidas, 2009; Maloney & Gallagher, 2011; Bemporad & Mancuso,

2010). One unique aspect in this work is the separation of these features though different image processing techniques, allowing us to carefully track each front individually with the different images and matching the appropriate geometry to the appropriate front. Figure (left) shows a white-light observation processed with an average background divided out of the image, leaving the ejecta as the most outstanding feature. Figure 3 (right) shows the same image processed using a running-difference technique, subtracting two consecutive images, which highlights the parts of the structure that are beyond the previous time step highlighting the sheath front.

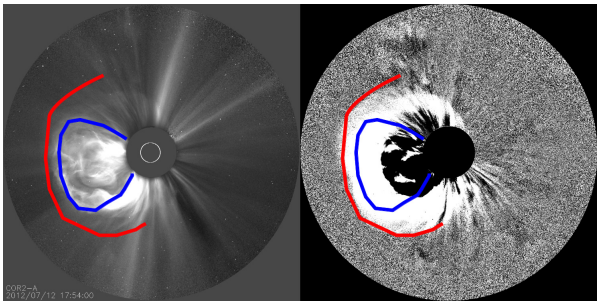

Figure 3: Tracking CME ejecta using the direct image (left) and the shock front using the difference image (right) Images from STEREO A COR2 at 17:54 UT on July 12, 2012 are used as an example. The ejecta is outlined in blue, the shock in red.

For both the shock and flux rope height-time measurement, I have been able to use an aerodynamic drag-based model to fit these measurements (Hess & Zhang, 2014). Most work with the drag model has just used a static value for the drag parameter Γ throughout the heliosphere. What is unique about my work is that I use a varying Γ as a function of distance, determined uniquely for each event from the measurements taken that allows the model to more accurately capture the solar wind environment that each eruption encounters.

Once Γ is known throughout the heliosphere, it can be used to create a more accurate representation of the drag model. In works using the drag model with a constant Γ, it is essentially a two point model between the initial CME height and detection at the Earth. In our method, starting with an initial height and velocity and using the Γ value at that height, the height and velocity at the next time step can be calculated. This process is done until the full propagation to the Earth is calculated.

Another unique feature in this work is the introduction of a correction factor for the curvature of the ejecta front and its evolution as the CME propagates. The height of the GSC

model is fitted to the nose of the CME, however, the CME might impact Earth anywhere along the curved front. Using the geometric formulas in Thernisien (2011), the difference in the height along the angular directions of the CME can be determined. Using this geometry, combined with arrival time at the Earth, a geometric correction based on the angular deviation of the propagation direction has been calculated and shown in Figure 4. The difference may seem minor, but a 7% difference for an average CME with a 500 km/s speed can mean a difference in arrival prediction of more than five hours, the current standard of prediction.

The geometry calculated from the GCS model cannot be used directly, as for all events studied it caused a lag in arrival prediction. This is because the GCS model assumes a self-similar expansion and fails to account for the evolution of the CME expansion profile that leads to a change of the curvature of the front and cross-sectional size of the flux rope. An addition to the GCS model that can take this kind of effect into account is just one of a number of possible improvements that could be added to the model. Currently the legs of the GCS geometry are fixed at the center of the Sun, which causes problems for the measurement of CMEs near the Sun and CMEs that are propagating non-radially. Allowing for the changing of these parameters, among others, would allow the GCS model to do more physical measurements of a CME eruption and interaction with the low corona.

One project that I would be able to work on as part of this proposal is an improvement on the GCS model, as the software is open source. Not only would this benefit the work I want to do by improving my measurement capabilities, but it would also benefit the community at large given the number of works that have utilized the GCS model as a measurement tool (Poomvises et al., 2010; Nieves-Chinchilla et al., 2012; Colaninno et al., 2013; Hess & Zhang, 2014; Shen et al., 2014).

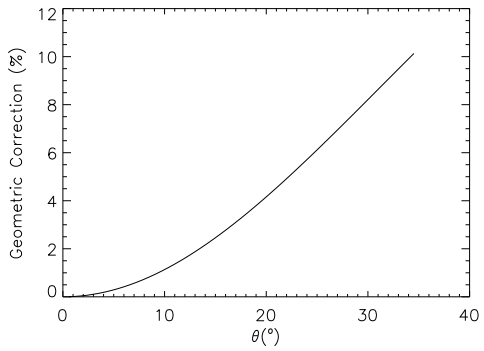

Figure 4: The effect of the geometric correction as a function of the θ angle between the CME nose and the Sun- Earth line.

With this much use by the heliospheric physics community, active development on the GCS model by someone with experience using the model, writing code in IDL and an understanding of the physics of CME evolution would greatly improve the model and increase its applicability.

The propagation model and geometry discussed previously were based solely on the flux rope ejecta. As I have explained, for a full understanding of the physics and space weather effects of a CME, it is necessary to separate the ejecta and sheath. The same technique that was successful for capturing the ejecta motion was unsuccessful at matching the sheath measurements to the in-situ detections, as the drag physics that governed the decelation of the CME are evidently not sufficient for modeling the sheath front physics. This is very likely due to the continued driving of the sheath front by its driver.

Using the reliable measurements of the sheath front in the heliosphere we propose to determine a physical model for the sheath. To determine the full sheath characteristics, the standoff-distance at each measurement was obtained by subtracting the ejecta height from the sheath height. For all events this provided a roughly linear profile for the standoff-distance in the domain of measurement. For now, the model in use is a linear fit of these standoff-distances, providing the standoff-distance as a function of height. Since the ejecta height is already known throughout the heliosphere, the ejecta height and the standoff-distance at any point in the heliosphere provides the sheath height as a function of distance.

This linear standoff-distance evolution is definitely an over-simplification, as the sheath size will not continue to grow infinitely. However, for faster CMEs that reach the Earth more quickly, this linear approximation does well at generating accurate arrivals. For slower CMEs, there tends to be a lag in the prediction, indicating there is a damping term in the standoff-distance growth as the CME propagates. For now, this method works to fit the data and create a basic evolution model, but will have to be physically improved.

As part of this proposal, I will improve theses physics as well as refine the geometry of the sheath. This can lead to work similar to what I plan to do with the GCS model in improving

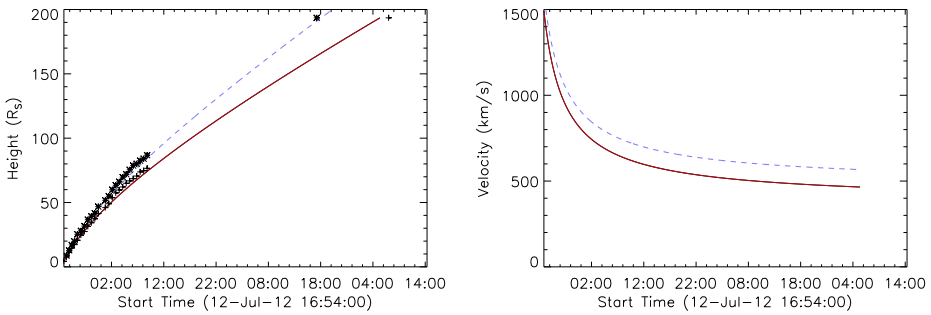

Figure 5: Left: The measurements for the ejecta (crosses) and sheath front (stars) for the July 2012 CME. The derived profiles for each front (red solid line, blue dashed line respectively) are also plotted. The maximum height in each plot is the arrival point of the front at ACE. Right: The velocity of the two fronts for the July 2012 CME. The sheath front is given by the dashed blue line, the ejecta by the solid blue line.

how the model is fit to the images, which can make measurement easier and more accurate. This is important both for tracking and modeling the sheath in the heliosphere and, as previously stated for determining when SEPs will be generated along magnetic field lines connected to the Earth, an important space weather concern. Just as with the GCS model, active development of this shock model would be of great importance for both scientific research and space weather forecasting applications.

Expected Results And Their Significance and Application

With our method, both fronts were fit independently and modeled. An example of the measurements with modeled heights and velocities for the July 2012 CME are plotted in Figure 5. To this point, this method has been used to accurately reconstruct the propagation and arrivals of 7 CMEs between 2010 and 2013, when STEREO was optimally positioned for observing Earth-directed transients. The results of these seven events are shown in Table 1 comparing the observed arrivals and velocities for each front.

For each of these events, which have varied initial speeds, encounter various solar wind environments and deviate as much as 30° in longitude from the Sun-Earth line, the method shows great success in recreating the ICME signature arrivals, and given the agreement between the model and in-situ arrivals also suggests that the model is accurately capturing

the propagation physics between the Sun and the Earth.

Obviously, given the science quality STEREO observations and ACE upstream solar wind speeds used to generate these models, this cannot truly be called prediction, and the model requires additional development and testing to be a true forecasting tool. However, given the consistent results across each event as well as the similarity between model and in-situ velocities, I can say that the model is accurately capturing the propagation of these events in the heliosphere, providing a good place to start for both the understanding of the physics of CME propagation and possibly an eventual forecasting tool, an important first step in improving the state of forecasting models.

These results can then be used to compare against forecasting models already in use to cross-validate. Currently we are working on a comparison with the MHD model Enlil (Odstrčil & Pizzo, 1999). By studying the parameter space of varying inputs to Enlil and comparing them to my measurements and results, it may be possible to determine the best values of these parameters for accurate CME prediction. I also plan to compare my model with the Eruptive Flux Rope model (Chen, 1996) which contains the aerodynamic drag force, as well as the Lorentz force driving the CME propagation. This comparison should allow for the addition of magnetic forces into the drag model, to improve the physical understanding that can be derived from the measurements, and possibly the predictive power of the model.

ICME Date[a]	ΔT_{SF}[b]	ΔT_{EJ}[b]	ΔV_{SF}[c]	ΔV_{EJ}[c]
04/05/2010	1.89	0.38	23.3	26.4
05/24/2010	5.69	2.52	96.3	38.1
09/14/2011	6.68	4.39	15.8	13.0
07/12/2012	0.84	1.51	24.8	22.4
09/28/2012	0.34	0.9	61.6	45.6
10/27/2012	4.99	0.28	24.5	19.0
03/15/2013	3.91	0.26	22.9	7.2
Average	3.47	1.46	38.5	24.5
RMS	1.58	0.76	17.9	12.9

Table 1: a- The date of the ICME arrival at ACE
b- The absolute value of the difference in hours between the predicted and observed arrival of the sheath (SF) and Ejecta(EJ)
c- The difference in velocity in km/s between the speed of each feature as predicted by the model and as compared to the average speed observed for each feature in-situ

Through these means, my work can improve all aspects of Coronal Mass Ejection research. I already demonstrate an ability to accurately measure a full CME structure in the heliosphere, and I propose to work to improve the tools upon which these measurements

for each front are based, furthering both my own work and that of the community. My work with the drag-based model has already shown an ability to fit these measurements and reproduce CME arrival at Earth, and alongside the eruptive flux rope model will help answer theoretical questions about how CMEs propagate. By comparing my measurements and models with with numerical models, the inputs to the simulations can be better parameterized, improving the quality of the models as well as prediction capabilities. With this approach combining observational data, analytical theory and numerical simulation, all the tools for CME study will be used together to produce a comprehensive and complete understanding of the forces governing CME evolution and have great benefits to multiple aspects of space weather forecasting.

Bibliography

Bala, R., Reiff, P., & Russell, C. T. 2015, Journal of Geophysical Research (Space Physics), 120, 3432

Bemporad, A. & Mancuso, S. 2010, ApJ, 720, 130

Burlaga, L., Sittler, E., Mariani, F., & Schwenn, R. 1981, J. Geophys. Res., 86(A8), 6673

Byrne, J. P., Long, D. M., Gallagher, P. T., Bloomfield, D. S., Maloney, S. A., McAteer, R. T. J., Morgan, H., & Habbal, S. R. 2013, A&A, 557, A96

Cargill, P. J. 2004, Sol. Phys., 221, 135

Chen, J. 1996, J. Geophys. Res., 101, 27499

Colaninno, R. C., Vourlidas, A., & Wu, C. C. 2013, Journal of Geophysical Research (Space Physics), 118, 6866

Gopalswamy, N., Xie, H., Akiyama, S., Mäkelä, P. A., & Yashiro, S. 2014, Earth, Planets, and Space, 66, 104

Hess, P. & Zhang, J. 2014, ApJ, 792, 49

Kozarev, K. A., Raymond, J. C., Lobzin, V. V., & Hammer, M. 2015, ApJ, 799, 167

Kwon, R.-Y., Zhang, J., & Olmedo, O. 2014, ApJ, 794, 148

Lepping, R. P., Jones, J. A., & Burlaga, L. F. 1990, J. Geophys. Res., 95, 11957

Li, Y., Luhmann, J. G., Lynch, B. J., & Kilpua, E. K. J. 2014, Journal of Geophysical Research (Space Physics), 119, 3237

Maloney, S. A. & Gallagher, P. T. 2011, ApJ, 736, L5

Nieves-Chinchilla, T., Colaninno, R., Vourlidas, A., Szabo, A., Lepping, R. P., Boardsen, S. A., Anderson, B. J., & Korth, H. 2012, Journal of Geophysical Research (Space Physics), 117, 6106

Odstrčil, D. & Pizzo, V. J. 1999, J. Geophys. Res., 104, 483

Ontiveros, V. & Vourlidas, A. 2009, ApJ, 693, 267

Poomvises, W., Zhang, J., & Olmedo, O. 2010, ApJ, 717, L159

Pulkkinen, T. 2007, Living Reviews in Solar Physics, 4, 1

Sheeley, N. R., Walters, J. H., Wang, Y.-M., & Howard, R. A. 1999, J. Geophys. Res., 104, 24739

Shen, C., Wang, Y., Pan, Z., Miao, B., Ye, P., & Wang, S. 2014, Journal of Geophysical Research (Space Physics), 119, 5107

Stone, R. G., Frandsen, A. M., Mewaldt, R. A., Christian, E. R., Margolies, D., Ormes, J. F., & Snow, F. 1998, Space Sci. Rev., 86, 1

Thernisien, A. 2011, ApJS, 194, 33

Thernisien, A., Vourlidas, A., & Howard, R. A. 2009, Sol. Phys., 256, 111

Thernisien, A. F. R., Howard, R. A., & Vourlidas, A. 2006, ApJ, 652, 763

Vourlidas, A., Lynch, B. J., Howard, R. A., & Li, Y. 2013, Sol. Phys., 284, 179

Vršnak, B., Žic, T., Vrbanec, D., Temmer, M., Rollett, T., Möstl, C., Veronig, A., Čalogović, J., Dumbović, M., Lulić, S., Moon, Y.-J., & Shanmugaraju, A. 2013, Sol. Phys., 285, 295

Zhang, J., Hess, P., & Poomvises, W. 2013, Sol. Phys., 284, 89

Zhang, J., Poomvises, W., & Richardson, I. G. 2008, Geophys. Res. Lett., 35, 2109